Developmental Biology 359 (2011) 82–94

Contents lists available at SciVerse ScienceDirect

Developmental Biology

journal homepage: www.elsevier.com/developmentalbiology

Myostatin-deficient medaka exhibit a double-muscling phenotype with hyperplasia and hypertrophy, which occur sequentially during post-hatch development

Shin-ichi Chisada [a,*], Hiroyuki Okamoto [b], Yoshihito Taniguchi [c,1], Yoshitaka Kimori [d], Atsushi Toyoda [e,2], Yoshiyuki Sakaki [e,3], Shunichi Takeda [c], Yasutoshi Yoshiura [a,*]

[a] Aquatic Animal Health Division, National Research Institute of Aquaculture, Fisheries Research Agency, 224-1 Hiruta, Tamaki, Mie, 519-0423, Japan
[b] Aquaculture Biology Division, National Research Institute of Aquaculture, Fisheries Research Agency, 224-1 Hiruta, Tamaki, Mie, 519-0423, Japan
[c] Department of Radiation Genetics, Graduate School of Medicine, Kyoto University, Yoshida Konoe, Sakyo-ku, Kyoto, 606-8501, Japan
[d] Center for Novel Science Initiatives, National Institutes of Natural Sciences, 4-3-13 Toranomon, Minato-ku, Tokyo, 105-0001, Japan
[e] Sequence Technology Team, RIKEN Genomic Sciences Center, 1-7-22 Suehiro, Tsurumi-ku, Yokohama, Kanagawa, 230-0045, Japan

ARTICLE INFO

Article history:
Received for publication 11 March 2011
Revised 28 June 2011
Accepted 30 August 2011
Available online 7 September 2011

Keywords:
Myostatin
Medaka
TILLING
Muscle
Hyperplasia
Hypertrophy

ABSTRACT

Myostatin (MSTN) functions as a negative regulator of skeletal muscle mass. In mammals, MSTN-deficient animals result in an increase of skeletal muscle mass with both hyperplasia and hypertrophy. A MSTN gene is highly conserved within the fish species, allowing speculation that MSTN-deficient fish could exhibit a double-muscled phenotype. Some strategies for blocking or knocking down MSTN in adult fish have been already performed; however, these fish show either only hyperplastic or hypertrophic growth in muscle fiber. Therefore, the role of MSTN in fish myogenesis during post-hatch growth remains unclear. To address this question, we have made MSTN-deficient medaka (*mstnC315Y*) by using the targeting induced local lesions in a genome method. *mstnC315Y* can reproduce and have the same survival period as WT medaka. Growth rates of WT and *mstnC315Y* were measured at juvenile (1–2 wk post-hatching), post-juvenile (3–7 wk post-hatching) and adult (8–16 wk post-hatching) stages. In addition, effects of MSTN on skeletal muscle differentiation were investigated at histological and molecular levels at each developmental stage. As a result, *mstnC315Y* show a significant increase in body weight from the post-juvenile to adult stage. Hyper-morphogenesis of skeletal muscle in *mstnC315Y* was accomplished due to hyperplastic growth from post-juvenile to early adult stage, followed by hypertrophic growth in the adult stage. Myf-5 and MyoD were up-regulated in *mstnC315Y* at the hyperplastic growth phase, while myogenin was highly expressed in *mstnC315Y* at the hypertrophic growth phase. These indicated that MSTN in medaka plays a dual role for muscle fiber development. In conclusion, MSTN in medaka regulates the number and size of muscle fiber in a temporally-controlled manner during posthatch growth.

Introduction

Myostatin (MSTN) or growth and differentiation factor-8 (GDF-8) is a member of the transforming growth factor-β (TGF-β) superfamily, and functions as a negative regulator of skeletal muscle mass (McPherron et al., 1997). MSTN-null mice generated by gene targeting show a drastic and widespread increase in skeletal muscle with a combination of hyperplasia and hypertrophy. Each muscle of mutant mice weighs 2–3 times compared to those of wild-type mice. Naturally occurring mutations in the MSTN gene have been identified in double-muscling cattle breeds (Kambadur et al., 1997; McPherron and Lee, 1997), dogs (Mosher et al., 2007) and even humans (Schuelke et al., 2004). MSTN protein is synthesized in skeletal muscle as a propeptide, which is processed by proteolytic cleavage to produce the mature form at the C-terminus. The C-terminal homodimer is known to be the biologically active molecule. The C-terminal amino acid sequence is highly conserved across mammalian and avian species (McPherron and Lee, 1997). Their identities are 95–100% among mouse, rat, human, porcine, chicken, turkey, baboon, bovine and ovine. Furthermore, in fish (for example, zebrafish, Atlantic salmon, sea perch, European seabass, bastard halibut and Chilean flounder), the C-terminal domain reaches identities higher than 88% comparing with mammalian MSTN (Delgado et al., 2008). According to these studies, there is a high possibility that the MSTN gene and its biological function should be conserved in vertebrates.

* Corresponding authors. Fax: +81 596 58 6413.
E-mail addresses: chisada@affrc.go.jp (S. Chisada), yoshiura@fra.affrc.go.jp (Y. Yoshiura).
[1] Present address: Department of Preventive Medicine and Public Health, Keio University, School of Medicine, 35 Shinanomachi, Shinjuku-ku, Tokyo, 160-8582, Japan.
[2] Present address: Comparative Genomics Laboratory, Center for Genetic Resource Information, National Institute of Genetics, Yata 1111, Mishima, Shizuoka, 411-8540, Japan.
[3] Present address: Toyohashi University of Technology, 1-1 Hibarigaoka, Tenpaku, Toyohashi, Aichi, 441-8580, Japan.

0012-1606/$ – see front matter © 2011 Elsevier Inc. All rights reserved.
doi:10.1016/j.ydbio.2011.08.027

Previous studies about the effects of MSTN in fish have demonstrated inconsistent phenotypes in body weight. Lee et al. (2009) reported that MSTN knock-down zebrafish using vector-based RNA interference exhibited a 1.4-fold increased body weight at 4 months. In contrast, Xu et al. (2003) showed that over-expression of MSTN prodomain as a dominant-negative form in zebrafish resulted in an only slightly increased body weight at 2.5 months. Sawatari et al. (2010) also revealed that over-expression of a dominant-negative form of MSTN in medaka did not change the body weight at 6 months. Therefore, it remains unclear whether blocking the MSTN function in fish leads to body weight gain. These reports also show conflicting phenotypes in muscle fibers. MSTN knock-down zebrafish resulted in only hypertrophy, while the over-expression of dominant-negative forms in zebrafish and medaka affected only hyperplasia. It is quite possible that these seemingly contradictory phenotypes in fibers are due to the incomplete inhibition of the MSTN signaling pathway. Thus, previous morphological evidence could not have demonstrated whether MSTN plays an inhibitory role in hyperplastic or hypertrophic muscle growth in fish. To accurately understand the MSTN function in fish, the generation of a completely MSTN-suppressed fish is required. Moreover, there is an important consideration in the evaluation of muscle growth in fish. Hyperplasia and hypertrophy in fish can continue during posthatch growth (Johnston, 1999; Rowe and Goldspink, 1969); however, in the studies reported previously, the effects of MSTN on myogenesis have been analyzed at single or a few points, but not throughout life. Therefore, there is some possibility that change of phenotypes is overlooked in transgenic fish for vector-based RNA interference and MSTN prodomain over-expression. To address these problems, further studies has been required using other techniques, which is able to completely inhibit MSTN function during posthatch growth.

In the current study, we made medaka with a MSTN deficient signaling pathway (called MSTN deficient medaka or *mstnC315Y* in the present report), corresponding to the naturally occurring mutation in double-muscled Piedmontese cattle (Kambadur et al., 1997), by targeting induced local lesions in the genome (TILLING) method (Taniguchi et al., 2006). *mstnC315Y* have the ability to reproduce and have the same survival period as WT medaka. These fish have allowed analysis of the effects of MSTN on myogenesis throughout life. As a result, the *mstnC315Y* shows a double-muscling phenotype with hyperplasia and hypertrophy. Moreover, we elucidated that MSTN in medaka regulated the number of muscle fibers at the post-juvenile stage and the size of those at the adult stage. Therefore, *mstnC315Y* mutant medaka provides an opportunity to elucidate the MSTN function in fish.

Materials and methods

Cloning of medaka MSTN gene

RNA was extracted from wild-type medaka larvae (Kyoto-Cab, a substrain of Cab) by RNeasy® Mini Kit (QIAGEN Sciences, MD, USA) according to the manufacturer's instructions. cDNA was synthesized using PowerScript (BD Biosciences Clontech, Palo Alto, CA, USA). To identify medaka MSTN gene orthologs, we used the basic local alignment search tool (BLAST) to search the medaka genome database (http://www.ensembl.org/Oryzias_latipes/blastview). Medaka MSTN cDNA sequences were then determined using a combination of RT-PCR and rapid amplification of cDNA ends (RACE). RACE products were generated using SMART™ RACE cDNA Amplification Kit (BD Biosciences Clontech). The 5′ RACE (1st: 5′-AGATCTTCACCTCAATGAACGGTTGCAG-3′, nest: 5′-TCTGCTGAGGTGACGGCTAAGTCATTTC-3′) and 3′ RACE primers (1st: 5′-GACGAGCATGCATCTACGGAGACAATTA-3′, nest: 5′-ATGGAGAGCCAAAGTGTTGCCTTTTCTC-3′) were used. The cDNA sequence was used to retrieve the genomic sequence from the draft medaka genome assembly.

Generation of MSTN mutant medaka

Generation of MSTN mutant medaka was carried out as described previously (Taniguchi et al., 2006). To find the mutations in the region of interest, the third exon of the medaka MSTN gene was screened using the forward primer #1 (5′-GGACAGCTGCCAAATAGTGC-3′) and reverse primer #1 (5′-AGGCTGACTGCTGCCTCTAC-3′) by PCR (92 °C for 60 s; 12 cycles of 92 °C for 20 s, 65 °C for 20 s with a decrement of 0.6 °C per cycle, 72 °C for 30 s; 20 cycles of 92 °C for 20 s, 58 °C for 20 s and 72 °C for 30 s; 72 °C for 180 s [ABI 9700 dual 384 well GeneAmp PCR system]). The PCR products were treated with an ExoSAP-IT kit (GE Healthcare). Sequencing reaction was then carried out using a BigDye terminator ver. 3 kit (Applied Biosystems) and the forward primer #1. Sequencing products cleaned up by ethanol precipitation were run on automated ABI 3730xl DNA analyzers (Applied Biosystems). *In vitro* fertilization was carried out using sperm with the desired mutation and the progeny were genotyped by sequencing. Heterozygous fish carrying the same mutation were back-crossed with wild-type medaka, at least 4 times. To verify the genotype from this incross, the DNA was amplified by PCR with forward primer #2 (5′-TCAGGAGAAGTAGGCAGCTGTG-3′) and reverse primer #2 (5′-CATGGAGGGGATCTTACCGTAG-3′). The 546-bp PCR product obtained was sequenced using the forward primer #3 (5′-ATGAGACCCTGACAGCCATC-3′). The resulting sequence chromatograms were analyzed for the expected single nucleotide polymorphism (guanine-to-adenine replacement) at one or both alleles (Fig. 2A). Wild-type fish (WT) and homozygous mutant line (*mstnC315Y*) obtained from the incross of heterozygous mutant parents were used for all the following experiments.

Nuclear protein preparation

Nuclear extract was prepared using the modified protocol previously described by (Lizotte et al., 2005). Skeletal muscle was frozen with liquid nitrogen and crushed into a fine powder. The obtained powder (200 mg) was mixed in 3 ml of the lysis buffer containing 50 mM Tris (pH 7.5), 250 mM NaCl, 5 mM EDTA, 0.1% NP-40, 1 mM NaF and 1:20 protease inhibitor cocktail (Complete Mini EDTA free, Roche Diagnostics K. K., Basel, Switzerland), and was homogenized at low speed for 1 min using a mechanical homogenizer (Physcotron NS-310E, Microtec Co., Ltd., Japan). The homogenate was centrifuged at 450×*g* and 4 °C for 15 min to remove tissue debris. The supernatant was mixed in an equal volume (3 ml) of the isotonic solution consisting of 10 mM Hepes (pH 7.5), 1.5 mM $MgCl_2$, 10 mM KCl, 0.5 mM dithiothreitol (DTT), 1 mM NaF and 1:20 protease inhibitor. Nuclei were pelleted by centrifugation at 2000×*g* and 4 °C for 15 min. The pellet was resuspended in the hypertonic solution consisting of 300 mM Hepes (pH 7.5), 30 mM $MgCl_2$, 1.4 M KCl, 0.5 mM DTT, 1 mM NaF and 1:20 protease inhibitor. To allow the nuclei to shrink, the resuspension was incubated on ice for 20 min. These were then centrifuged at 2000×*g* and 4 °C for 15 min. The final pellet was resuspended in the storage solution containing 20 mM Hepes (pH 7.5), 420 mM NaCl, 1.5 mM $MgCl_2$, 0.2 mM EDTA, 0.5 mM DTT, 25% (v/v) glycerol, 1 mM NaF and 1:20 protease inhibitor. The protein concentration was determined with the BCA Protein Assay (Pierce, IL, USA).

SDS-PAGE and western blotting

Nuclear proteins were separated by sodium dodecyl sulfate-polyacrylamide gel electrophoresis (SDS-PAGE). This technique was performed using 4% (w/v) acrylamide stacking gel followed by a 5–20% gradient separation gel. Proteins were transferred to a PVDF membrane (0.2 μm Pall Fluoro Trans® W membranes, Pall Corp., MI, USA). Firstly, the membrane was washed with TBS (20 mM Tris–HCl, pH 7.5, 150 mM NaCl) for 5 min and then blocked with blocking

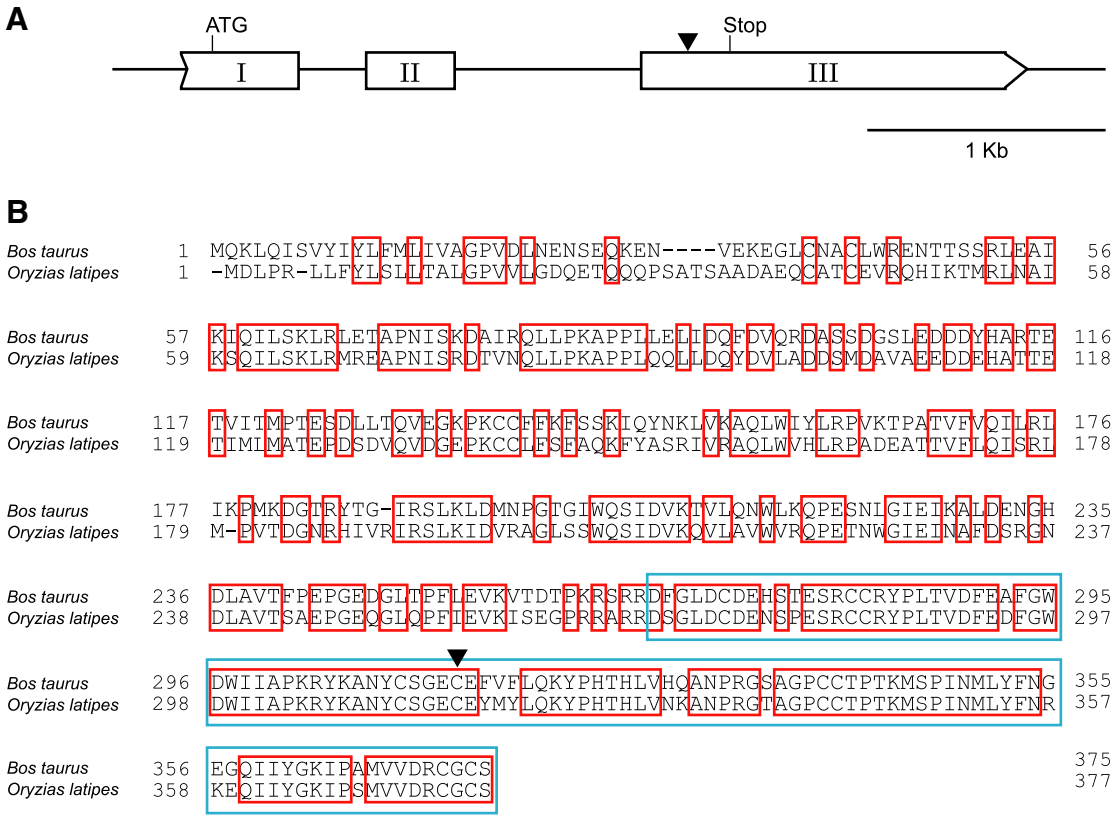

Fig. 1. Medaka MSTN profiles. (A) Genome structure of medaka *MSTN* gene (3551 bp). White boxes indicate each exon (with the Greek numeral representing the number of exon) and bars represent each intron. (B) Sequence alignment of bovine and Kyoto-Cab medaka MSTN protein. Amino acids conserved across the two species are outlined in red. The medaka MSTN amino-acid sequence has a 61.3% identity to bovine MSTN. The C-terminal protein, which is an active peptide, is outlined in light blue. The medaka C-terminal region has an 88.1% identity to bovine MSTN. Black triangles in panels A and B indicate the amino acid responsible for the phenotype in this study.

solution (1% ECL plus Blocking Agent [GE Healthcare Co., Ltd., UK] in TBS containing 0.05% (v/v) Tween20) for 1 h at room temperature (RT). The blocking solution was also used as dilution solutions for antibodies. Next, the membrane was incubated overnight at 4 °C with the following primary antibodies; anti-phospho Smad2 (1:1000, Cell Signaling Technology, Inc., MA, USA), anti-histone H2B

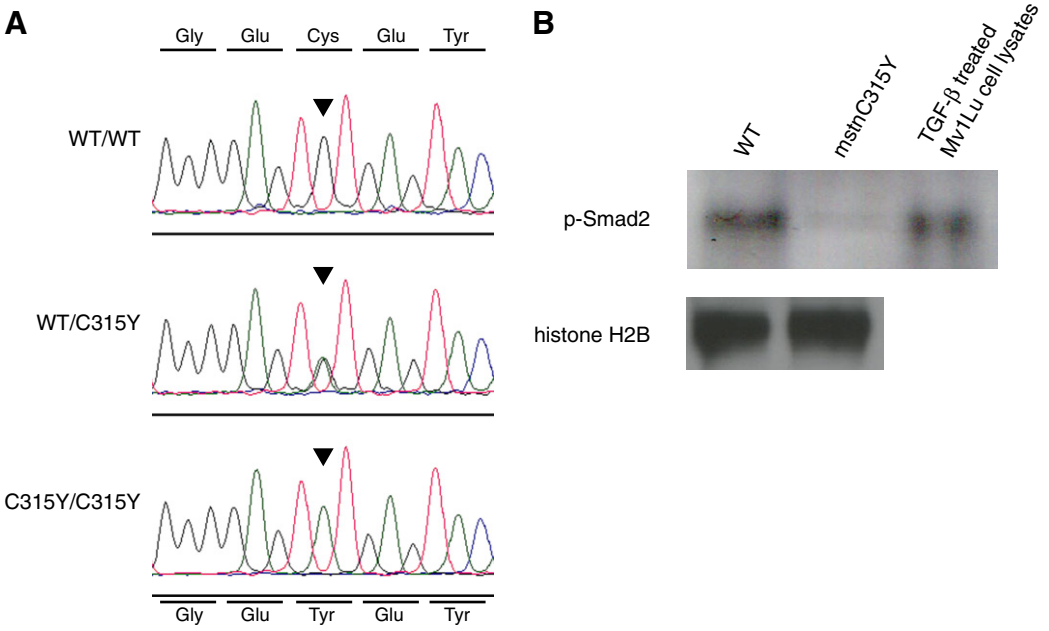

Fig. 2. Generation of *mstnC315Y* medaka. (A) Sequence data for each genotype. Lines in green, red, black and blue indicate adenine, thymine, guanine and cytosine, respectively. Three-letter amino-acid codes show the resulting transcript. Top figure illustrates WT medaka sequence, while middle and bottom figures illustrate heterozygous and homozygous C315Y mutation, respectively. Guanine to adenine nucleotide transition causes an amino-acid change from Cys to Tyr at amino acid 315 (black triangles). (B) Demonstration of deficient medaka for the MSTN signaling pathway. Phosphorylated Smad2 in nuclear proteins were targeted and detected with western blotting. Nucleus protein were obtained from muscles of WT (left lane) and *mstnC315Y* (middle lane) at 16 wk post-hatching. Upper figure shows decreased expression of phosphorylated Smad2 in *mstnC315Y*. TGF-β treated Mv1Lu cell lysates were used as positive control of phosphorylated Smad2 for western blotting (right lane). Lower figure shows histone H2B used as a loading control.

(1:1000, Millipore Corp., MA, USA), and was washed twice with TBS containing 0.05% (v/v) Tween 20 for 20 min. Immunoreactive bands were detected with the secondary antibody (HRP-conjugated goat anti-rabbit IgG antibody, GE) and ECL detection reagent (GE) according to the manufacturer's instructions. Chemiluminescent signal was visualized by exposing to hyperfilm ECL (GE). TGF-β treated Mv1Lu cell lysates (Santa Cruz Biotechnology, Inc., CA, USA) were used as a positive control for phosphorylated Smad2 protein. Equal loading of the proteins was confirmed with an anti-histone H2B antibody.

Fish husbandry

Medaka (*Oryzias latipes*) were maintained in aerated freshwater under a 14 h light/10 h dark photoperiod at a water temperature of 27 ± 1 °C. In this condition, they sexually matured and spawned daily. Eggs were incubated in 0.0001% methylene blue until they hatched. Hatched larvae were transferred to a petri dish (diameter; 90 mm) and fed with paramecium. At 7–10 day after hatching, they were transferred to each plastic rearing container (2 L or 5 L) and fed with newly hatched *Artemia* nauplii and commercial powder feeds for fish fry from juvenile to adult. Feeding was carried out five times a day, so that all fish experienced *ad libitum* food availability.

Growth evaluation

Ten breeding pairs in WT and *mstnC315Y* groups were randomly chosen and reared in plastic rearing containers. Approximately 300 eggs in each group were obtained simultaneously. Of hatched larvae in each group, 200 larvae were reared until 5 wk post-hatching as described above. After 5 wk post-hatching, fish were transferred to large tanks (150 L) to avoid adverse effects of the rearing density on growth. Fish in both groups were fed the same amount at the same time throughout the experimental period. To analyze growth rates in WT and *mstnC315Y*, both of standard length and body weight were measured according to the following procedure. Ten fish were randomly sampled from each group at 1, 2, 3, 4, 5, 7, 9, 12, and 16 wk post-hatching. After 7 wk post-hatching (sexually mature), all samplings were conducted to have an equal sex ratio (5 males and 5 females) in consideration of the sexual difference in the growth. Fish were anesthetized using 0.003% eugenol (FA100, Tanabe Seiyaku Co., Ltd., Japan) and photographed using a digital microscope (Focus-Studio 1400, Nakaden Co., Ltd., Japan). Standard length (*SL*: the length of a fish measured from the tip of the snout to the posterior end of the last vertebra) was measured from the captured digital image using image analysis software (Image-Pro® Plus v4.5.1, Media Cybernetics, Inc., MD, USA). For the purpose of measuring body weight (*BW*), BD Falcon cell strainer tubes (Becton Dickinson Co., NJ, USA) were used. Fish were individually put on nylon membrane of cell strainer (BD). The tubes were briefly centrifuged at $1500 \times g$ for 1 min; from these results the extra water on the body surface was removed under the same conditions, and body weight could be accurately measured. Condition factor (*K*) was calculated as $BW/SL^3 \times 10^2$ (*BW*: body weight in mg, *SL*: standard length in mm).

Quantitative PCR analysis

Gene expression analysis of myogenic regulatory factors (MRFs: MyoD, Myf5, and myogenin) in skeletal muscle was performed with quantitative PCR as described in the MIQE guidelines (Bustin et al., 2009). Skeletal muscle was sampled from three individuals of *mstnC315Y* and WT at four different developmental stages (2, 5, 8, and 16 wk post-hatching) from juvenile to adult as representatives for gene expression analysis. After fish were anesthetized using 0.003% eugenol, all fins and the head containing the operculum were cut off, and then the abdominal viscera were removed from fish. Skeletal muscle was immediately fixed using RNAlater solution (Ambion, Austin, TX, USA) for 5 h at room temperature. From 2 wk post-hatching fish, whole skeletal muscle (approximately 1.0 mg) was stored in RNAlater solution. From 5, 8, and 16 wk post-hatching, muscular portion containing the anus (approximately 20 mg) was removed and stored in RNAlater solution. Total RNA was extracted using RNeasy® Mini Kit (QIAGEN) and RNA in the extracted samples was quantified using spectrophotometry (NanoDrop, Thermo Scientific). Genome DNA elimination and reverse transcription was performed with the extracted samples containing 500 ng total RNA using QuantiTect® Reverse transcription Kit (QIAGEN) according to the manufacturer's protocol. Quantitative PCR was performed in a total of 25 μl containing 12. 5 μl of SYBR® *Premix EX Taq*™ (Takara Bio Inc., Shiga, Japan), 0.5 μl of ROX Reference Dye II (Takara), 150 ng of cDNA (1 μl of 1:10 dilution of the reverse transcription) as a template, and each primer at a final concentration of 0.2 μM. Using Primer3 programs on the web (source code available at http://fokker.wi.mit.edu/primer3/), primer sets for the quantitative PCR of medaka MRFs were designed in the nucleotide sequence of medaka MyoD (Ensembl Gene ID: ENSORLG00000000694), Myf5 (Ensembl Gene ID: ENSORLG00000016257), and myogenin (Ensembl Gene ID: ENSORLG00000015906) on the Ensembl Genome Browser (http://www.ensembl.org). The primer sets and amplicon sizes were as follows, Myf5: 5′-CTGAGCCTGGAAGTCCTCTGTC-3′ and 5′-GGCTGTCTTGTTGTCCAAACTC-3′, yielding a fragment of 137 bp; MyoD: 5′-CTCCAACTGCTCTGACGGAAT-3′ and 5′-ACTGGAGACGACGGAGCTG-3′, yielding a fragment of 142 bp; myogenin: 5′-TCAACCAGCAGGACACAGAGAC-3′ and 5′-CACCAACACTCAGAAGATCCTC-3′, yielding a fragment of 186 bp. MRFs mRNA levels were normalized by EF-1α with primer set (5′-CTGCAGGACGTCTACAAAATCG-3 and 5′-TGGTTCAGGATGATGACCTGAG-3′′ , yielding a fragment of 299 bp) as the reference gene. The fragment length of each sample was checked by agarose gel electrophoresis. Each PCR reaction in the quantitative PCR analysis was conducted in triplicate with an initial denaturation step of 10 s at 95 °C followed by an amplification of the target cDNA (40 cycles at 95 °C for 5 s and 60 °C for 20 s) using Mx3005P Real-time QPCR System (Stratagene, CA, USA). In this method, PCR-efficiency was calculated using the standard curve generated by plotting the threshold cycle vs. the known dilution of each PCR product (Myf5, 102.4%; MyoD, 98.6%; myogenin, 102.7%; EF-1α, 100.0% amplification efficiency). This allowed confirmation of the validity of each primer set in this analysis. There was no difference in EF-1α mRNA expression between *mstnC315Y* and WT medaka at each developmental stage. The results are presented as changes in relative expression normalized to the reference gene using the $2^{-(\Delta\Delta Ct)}$ method described by (Pfaffl, 2001).

Histological analysis

Skeletal muscle was sampled from three individuals of *mstnC315Y* and WT at four different developmental stages (2, 5, 8, and 16 wk post-hatching) from juvenile to adult as representatives for histological analysis. Each sample was fixed in Davidson's fixative solution (33% EtOH, 22% formalin, and 11.5% acetic acid in distilled water (DW)) for 24 h at RT. After washing twice with DW, samples were decalcified by EDTA solution containing 50 mM Tris (pH 8.3) and 400 mM EDTA for 24 h at RT and dehydrated, paraffin-embedded using Leica EG 1160 (Leica Microsystems, Germany), and serially sectioned at 4 μm thickness using Leica RM2145 (Leica). The sections were mounted on glass slides (Superfrost® micro slide glass, Matsunami Co., Ltd., Japan) covered with egg albumen and stained with Mayer's hematoxylin (Sigma-Aldrich, Inc., MO, USA) and eosin (Wako, Co., Ltd., Japan). Cross section at the position of pelvic fins was used for counting the number of muscle fibers. Counting area was described in Fig. 5A. Cellularity was calculated as the number of fibers per cross-sectional muscle area, and used for evaluating fiber

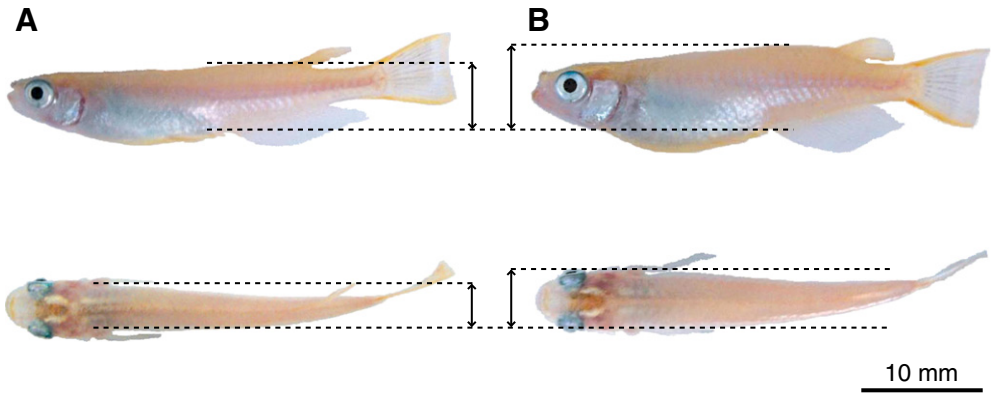

Fig. 3. Morphology of WT and *mstnC315Y* medaka. (A) Side (upper) and overhead (under) view of WT. (B) Side (upper) and overhead (under) view of *mstnC315Y*. Double-headed arrows show height and width of body. *mstnC315Y* exhibited higher and wider body trunk than WT. Both medaka were sampled at 16 wk post-hatching. Scale bar; 10 mm.

size. The lower cellularity means that each fiber in a cross section is larger. The muscle area was measured from the captured digital image using Image-Pro® Plus v4.5.1.

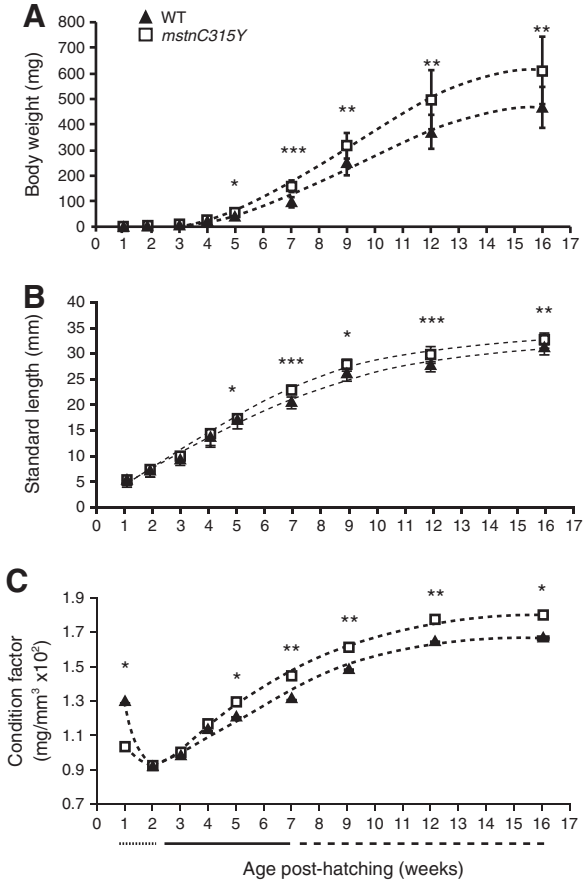

Fig. 4. Growth curves from juvenile to adult stage. Measurement of body weight (*BW*), standard length (*SL*) and condition factor (*K*) as growth indices in WT (black triangles) and *mstnC315Y* (white squares) medaka. *K* value was calculated as $10^2 \times BW/SL^3$ for each. Data were sampled at 1, 2, 3, 4, 5, 7, 9, 12 and 16 wk post-hatching, respectively. (A) Growth curve of *BW* for each group. $BW_{mstnC315Y}$ significantly increased at 5 wk post-hatching for the first time ($BW_{WT} = 45.2 \pm 9.4$ mg, $BW_{mstnC315Y} = 55.5 \pm 9.8$ mg). Each *BW* value plateaued at 16 wk post-hatching with significant differences in body weight between the two groups ($BW_{WT} = 467.2 \pm 82.0$ mg, $BW_{mstnC315Y} = 609.4 \pm 131.2$ mg). (B) Growth curve of *SL* for each group. $SL_{mstnC315Y}$ was significantly longer than SL_{WT} from 5 to 16 wk post-hatching. (C) Curve of *K* for each group. *K* values in both groups showed significant differences from 5 to 16 wk post-hatching. Broken lines in all panels show fitted curves. The dots, black, and broken lines under *t*-axis (age post-hatching) indicate the juvenile, post-juvenile and adult stage, respectively. Values are means ± SEM (n = 10 per sample point in all panels). $^*p<0.05$, $^{**}p<0.01$, and $^{***}p<0.001$, respectively.

Morphological image processing for quantitative analysis of muscle fiber image

The size distribution of muscle fibers was analyzed based on extended morphological image processing (Kimori et al., 2007, 2010). Original images (32-bit color images) of cross sections were first converted to 8-bit grayscale images. In order to reduce speckle noise and to improve the signal-to-noise-ratio of images, the grayscale images were applied to Gaussian smoothing filter. Additionally, the edges of muscle fiber region were enhanced by top-hat filtering (Meyer, 1979). These enhanced images were binarized by a local thresholding method (Niblack, 1986). Muscle fiber regions were segmented by watershed transform (Meyer and Beucher, 1990), and then the segmented region was represented as the region enclosed by a 1-pixel-wide contour line. Finally, each region was calculated as the size of its muscle fiber.

Immunohistochemical staining

Localization of PCNA (proliferation cell nuclear antigen)-positive cells in muscle fibers was analyzed by an immunohistochemical procedure. Coronal section of skeletal muscle was used for immunohistochemical analysis of PCNA. Observed area is described in Fig. 5B. The sections were treated with 3% H_2O_2 aq. for 30 min at RT, and were incubated with a monoclonal mouse anti-PCNA (Clone PC10) (Thermo Scientific, CA, USA) overnight at 4 °C. Anti-PCNA antibody was diluted 1:300 with Can Get Signal immunostain immunoreactions enhancer solution A (Toyobo Co., Ltd., Japan). After washing twice with TBS, sections were incubated with peroxidase-labeled anti-rabbit or anti-mouse antibody (Histofine Simplestain Max PO; Nichirei, Co., Ltd., Japan) for 30 min at RT. Peroxidase activity was detected with diaminobenzine (DAB; Sigma-Aldrich).

Statistical analysis

Data were expressed as mean ± standard error of the mean (SEM). Results were statistically evaluated for significance using the *t*-test between *mstnC315Y* and WT groups for all analyses of growth, fiber size and number, and expression of MRF mRNAs. Differences were considered significant when $p<0.05$.

Results

Cloning of medaka MSTN

Only a single ortholog of the mammalian MSTN gene was identified (by the BLAST search) in the medaka genome. The medaka MSTN gene has 3 exons and encodes a protein consisting of 377

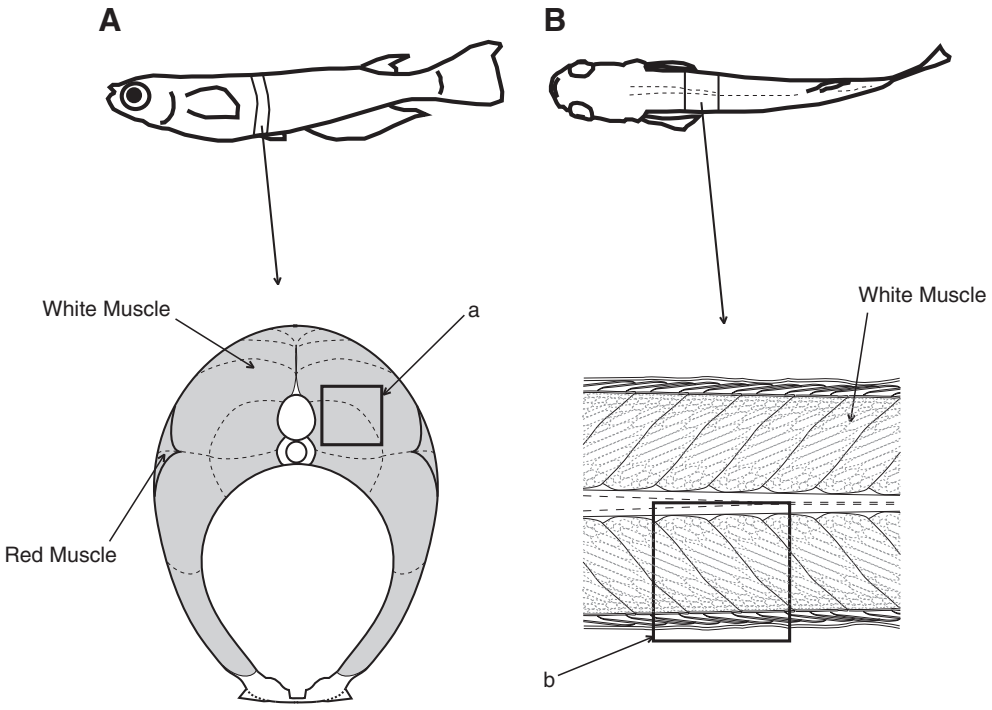

Fig. 5. Diagrams of body areas of medaka used for histological analysis. (A) Ventral cross-sectional area. Shaded gray area was used for counting fiber numbers and measuring muscle area. Square *a* is shown as photographs in Fig. 6. (B) Horizontal cross-sectional area. All the area was used for immunohistochemical analysis. Square *b* is indicated as photographs in Fig. 10.

amino acids (Fig. 1). The medaka MSTN amino acid sequence has a 61.3% identity to bovine MSTN. The C-terminal protein is an active peptide. The medaka C-terminal region has an 88.1% identity with the bovine C-terminal region.

Generation of MSTN mutant medaka

To generate MSTN mutant medaka, we targeted exon 3 of the MSTN gene for nucleotide sequencing. We sequenced the genomes of 5760 samples obtained from ENU-mutagenized medaka. We identified a C315Y-substituted mutant, corresponding to naturally occurring mutation (C313Y) in double-muscled Piedmontese cattle (Kambadur et al., 1997) (a black triangle in Figs. 1A and B, and underlined in Table 1). From the incross of heterozygous C315Y mutant parents, we obtained the expected numbers of wild-type fish (WT), heterozygous mutants, and homozygous mutants (*mstnC315Y*) (Fig. 2A). Piedmontese cattle have a double muscled phenotype due to a point mutation in the MSTN gene causing a substitution of tyrosine for cysteine (C313Y) in the signaling portion of the protein. In order to confirm whether *mstnC315Y* have lost the MSTN function, we examined the level of phosphorylated Smad2 in the nuclear proteins from skeletal muscle between WT and *mstnC315Y* medaka by western blotting. As expected, *mstnC315Y* had minimal phosphorylation of Smad2 in skeletal muscle whereas WT showed a distinct band of phosphorylated Smad2 (Fig. 2B). This revealed that the *mstnC315Y* mutation had blocked the MSTN signal pathway in skeletal muscle, indicating that a point mutation in the MSTN gene causing a substitution of tyrosine for cysteine (C315Y) resulted in the loss of MSTN function in medaka. We therefore concluded that we had succeeded in generating MSTN-deficient medaka.

Table 1
List of MSTN mutations from our TILLING library showing mutated nucleotides and resulting changes of the transcript.

DNA sequence	Amino acid substitution
TGAGGTGAAG (A>G) TCTCAGAGGG	I 259V
GTCCCGTTGC (T>A) GCCGCTACCC	C284S
TCTGGGGAGT (G>A) TGAGTACATG	C315Y
GTGTGAGTAC (A>C) TGTACTTGCA	M318L
ACCCACCAAG (A>T) TGTCGCCCAT	M347L
ACCCACCAAG (A>G) TGTCGCCCAT	M347V
CCCATCAACA (T>C) GCTCTACTTT	M352T
TAAGATCCCC (T>C) CCATGGTGGT	S368P

(A>B): A is the nucleotide of wild-type Kyoto-cab and B is the nucleotide of the mutant. There were eight types of mutation in the exon 3 and all mutations were amino acid substitutions. The mutation we selected (C315Y) is underlined.

Morphology and growth evaluation of MSTN mutant medaka

MSTN loss-of-function or several MSTN mutations cause increased muscle mass in a variety of mammals. We examined the morphology of *mstnC315Y* medaka at the adult stage. As shown in Fig. 3, *mstnC315Y* medaka exhibited a higher and wider body trunk than WT, implying that *mstnC315Y* medaka had an increased muscle mass. Growth rates of WT and *mstnC315Y* medaka throughout life were measured from juvenile to adult (juvenile stage: 1–2 wk post-hatching, post-juvenile stage: 3–7 wk post-hatching, adult stage: 8–16 wk post-hatching) as described in Materials and methods. There was no difference in body weight (*BW*) between the two groups from 1 to 4 wk post-hatching; however, the increasing *BW* in *mstnC315Y* accelerated from 5 wk post-hatching up to 12 wk post-hatching, resulting that there was a significant difference between the two groups from 5 to 16 wk post-hatching (Fig. 4A). At 16 wk post-hatching, *mstnC315Y* showed a 1.3 fold weight gain ($BW_{mstnC315Y} = 609.4 \pm 131.2$ mg) compared to WT ($BW_{WT} = 467.2 \pm 82.0$ mg). Both growth curves of standard length (*SL*) in WT and *mstnC315Y* were similar to each other although *mstnC315Y* showed slightly higher values than WT after 5 wk post-

juvenile stage (Fig. 4B). Since the increase of $BW_{mstnC315Y}$ might be considered due to an increase of $SL_{mstnC315Y}$, condition factors ($K = 10^2 \times BW/SL^3$) were used. Fig. 4C showed that $K_{mstnC315Y}$ values were significantly higher than K_{WT} from 5 to 16 wk post-hatching, indicating that *mstnC315Y* medaka induced an increased body weight per standard length after 5 wk post-hatching.

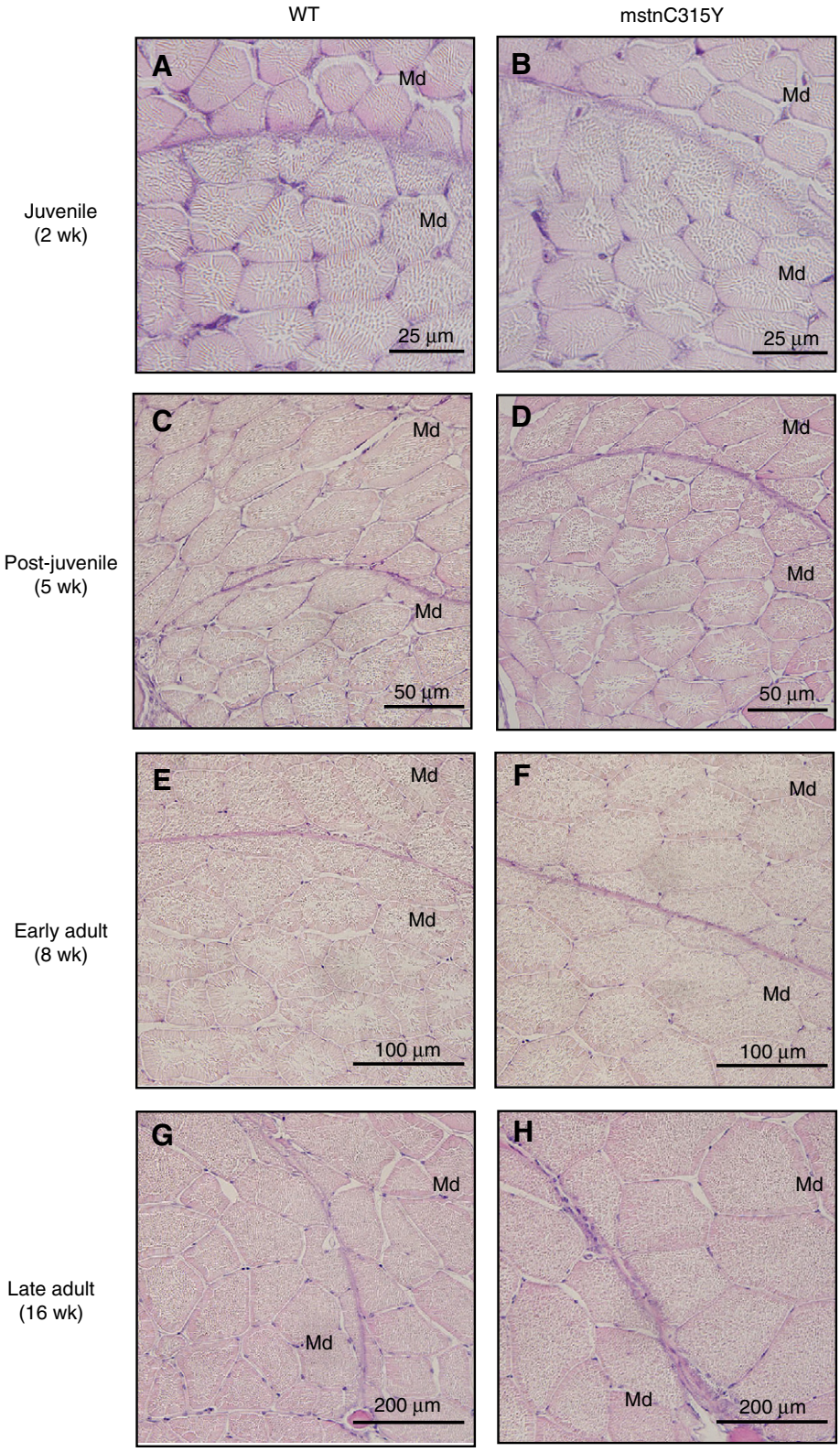

Fig. 6. Muscle fiber development in size during posthatch growth. Histological analysis of muscle fiber in WT (A, C, E, and G) and *mstnC315Y* (B, D, F and H) medaka. Cross-sectional area is described in Fig. 5A. Cross-sections were stained with hematoxylin–eosin. (A and B) Muscle fibers at juvenile stage (2 wk post-hatching). (C and D) Muscle fibers at post-juvenile stage (5 wk post-hatching). (E and F) Muscle fibers at early adult stage (8 wk post-hatching). (G and H) Muscle fibers at late adult stage (16 wk post-hatching). There was no difference in fiber size between WT and *mstnC315Y* until the post-juvenile stage, while fiber size in *mstnC315Y* was larger than that in WT at the adult stage. Scale bars; 25 μm for (A) and (B); 50 μm for (C) and (D); 100 μm for (E) and (F); 200 μm for (G) and (H). Md; M. latero-dorsalis.

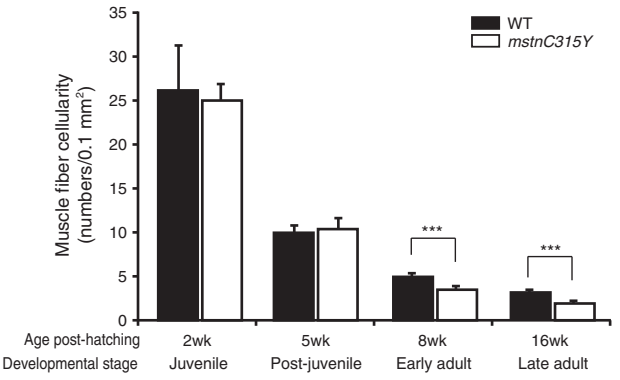

Fig. 7. Cellularity as an indicator of muscle fiber size. A quantitative analysis for the size of muscle fiber in WT (black columns) and *mstnC315Y* (white columns) medaka. Cellularity was calculated as the number of fibers/cross-sectional muscle area. Measurement area is described in Fig. 5A. Lower cellularity indicates a larger size in muscle fiber. There was minimal difference in cellularity between WT and *mstnC315Y* in the juvenile and post-juvenile stage, while cellularity in *mstnC315Y* was lower than that in WT in the adult stages. Values are means ± SEM ($n = 3$, at all sample points). $^{***}p < 0.001$.

Loss of MSTN function induces hypertrophy of muscle fibers in skeletal muscle during the adult stage

To elucidate the effect of deficient MSTN on skeletal muscle, we performed histological observations and two quantitative analyses of muscle fibers in skeletal muscle of WT and *mstnC315Y* medaka. At the microscopic level, there was seemingly no difference in fiber size between the two groups at juvenile (2 wk post-hatching, Figs. 6A and B) and post-juvenile stages (5 wk post-hatching, Figs. 6C and D). At the late adult stage (16 wk post-hatching, Figs. 6G and H), muscle fibers of *mstnC315Y* were visibly larger than those of WT. Next, cellularity (muscle fiber density) was used for a quantitative comparison of fiber size. Lower values of cellularity mean that each fiber in a cross section is larger. Fig. 7 shows that there was little difference in cellularity between WT and *mstnC315Y* at the juvenile and post-juvenile stages, suggesting that at these stages the fibers were the same size. Although the difference in fiber size at the early adult stage (8 wk post-hatching) was difficult to explain by only microscopic observations, cellularities demonstrated a statistically-significant difference in fiber size between the two groups at this stage. The cellularity in *mstnC315Y* at the early adult stage exhibited a significantly lower value than that in WT (Fig. 7), indicating that *mstnC315Y* at this stage had larger sized muscle fibers than WT. At the late adult stage, the lower cellularity supported that hypertrophy was induced in muscle fibers of *mstnC315Y* at this stage. The size of each muscle fiber was further analyzed using another method. The morphological image processing can provide quantitative analysis of muscle fiber size by measuring each fiber area (*FA*). Fig. 8 shows one pair of comparisons of the distribution and median value of *FA* between WT and *mstnC315Y*. At the juvenile and post-juvenile stages, median values of *FA* in *mstnC315Y* were not higher than WT (median value of $FA_{WT} = 282.1\ \mu m^2$, median value of $FA_{mstnC315Y} = 250.0\ \mu m^2$ at the juvenile stage; median value of $FA_{WT} = 727.5\ \mu m^2$, median value of $FA_{mstnC315Y} = 718.4\ \mu m^2$ at the post-juvenile stage). Maximum areas of *mstnC315Y* were much larger than those of WT (max $FA_{WT} = 993.0\ \mu m^2$, max $FA_{mstnC315Y} = 1556.1\ \mu m^2$ at the juvenile stage; max $FA_{WT} = 3054.5\ \mu m^2$, max $FA_{mstnC315Y} = 3754.6\ \mu m^2$ at the post-juvenile stage), while the number of small fibers in *mstnC315Y* were more than that in WT. Therefore, muscle fiber development in *mstnC315Y* did not exhibit marked hypertrophy compared to that in WT at the juvenile and post-juvenile stages, although fiber size in both WT and *mstnC315Y* medaka was growing at the juvenile and post-juvenile stages. At the early and late adult stages, there was a large difference in the median values of *FA* between WT and *mstnC315Y* (median value of $FA_{WT} = 1607.1\ \mu m^2$, median value of $FA_{mstnC315Y} = 2008.4\ \mu m^2$ at the early adult stage; median value of $FA_{WT} = 1627.8\ \mu m^2$, median value of $FA_{mstnC315Y} = 2186.3\ \mu m^2$ at the late adult stage). Furthermore, the fiber area distributions of *mstnC315Y* shifted to the right of WT at

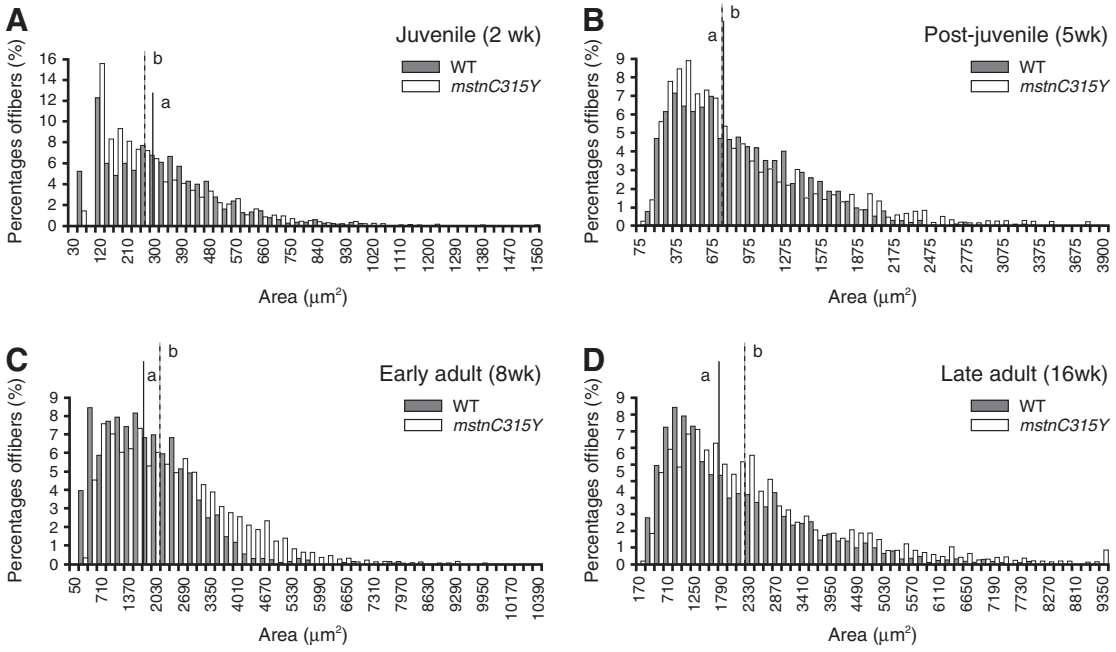

Fig. 8. Distribution analysis of muscle fiber area. Quantitative analysis for cross-sectional fiber area in WT (gray columns) and *mstnC315Y* (white columns) medaka. Cross-sectional fiber area was measured at juvenile (A), post-juvenile (B), early adult (C), and late adult (D) stages, using morphological image processing. Black line *a* and broken line *b* in all panels show median values of fiber area of WT and *mstnC315Y*, respectively. At the juvenile stage, median value of *FA* in *mstnC315Y* was lower than that in WT (median value of $FA_{WT} = 282.1\ \mu m^2$, median value of $FA_{mstnC315Y} = 250.0\ \mu m^2$). At the post-juvenile stage, median value of *FA* in *mstnC315Y* was about the same value as WT (median value of $FA_{WT} = 727.5\ \mu m^2$, median value of $FA_{mstnC315Y} = 718.4\ \mu m^2$). At the adult stage, median values of *FA* in *mstnC315Y* were larger than those in WT (median value of $FA_{WT} = 1607.1\ \mu m^2$ < median value of $FA_{mstnC315Y} = 2008.4\ \mu m^2$ at the early adult stage; median value of $FA_{WT} = 1627.8\ \mu m^2$ < median value of $FA_{mstnC315Y} = 2186.3\ \mu m^2$ at the late adult stage). The result was confirmed by repeated analysis using another fish of WT and *mstnC315Y* at each developmental stage.

these stages. These results clearly show that the muscle fiber size of *mstnC315Y* was larger than that of WT at the adult stage. The result from the morphological image processing was confirmed by repeated analysis using another fish of WT and *mstnC315Y* at each developmental stage. Therefore, we conclude that loss of the MSTN function induces hypertrophy of muscle fibers in skeletal muscles at the adult stage.

Loss of MSTN function induces hyperplasia of muscle fibers in skeletal muscle from the post-juvenile stage to early adult stage

Muscle fiber number in WT increased linearly up to the post-juvenile stage (5 wk post-hatching) and reached a plateau during the adult stage (8 and 16 wk post-hatching), whereas that in *mstnC315Y* increased up to the early adult stage (8 wk post-hatching) and reached a plateau at the late adult stage (16 wk post-hatching) (Fig. 9A). Furthermore, *mstnC315Y* had a larger number of muscle fibers than WT at all stages, and showed a 1.3-fold increase in fiber number at the adult stage, indicating that a loss of the MSTN function caused hyperplasia of muscle fibers. The relation between *SL* and fiber number is illustrated in Fig. 9B. Muscle fiber number in WT increased linearly up to 15 mm in *SL*, and reached a plateau value (1912.4 ± 129.3 fibers). Muscle fiber number in *mstnC315Y* increased approximately linearly up to 20 mm, and reached a plateau value (2551.7 ± 201.9 fibers) with 33% increase compared to WT. At the post-juvenile stage (15 mm in *SL*), muscle fiber number in WT reached a plateau, whereas that in *mstnC315Y* was increasing linearly at this stage. Therefore, we confirmed the proliferation of myogenic cells in *mstnC315Y* by immunohistochemical analysis for proliferation cell nuclear antigen (PCNA). At the post-juvenile stage (15 mm in SL), *mstnC315Y* still have many PCNA-positive myocytes although WT rarely have PCNA-positive myocytes (Figs. 10A and B), indicating that in *mstnC315Y*, muscle cells still proliferated at the post-juvenile stage. At the early adult stage (20 mm in *SL*), there is no PCNA-positive myocytes in both WT and *mstnC315Y* (Figs. 10E and F). These results indicate that loss of MSTN function induces hyperplasia of muscle fibers in skeletal muscle from the post-juvenile stage to early adult stage.

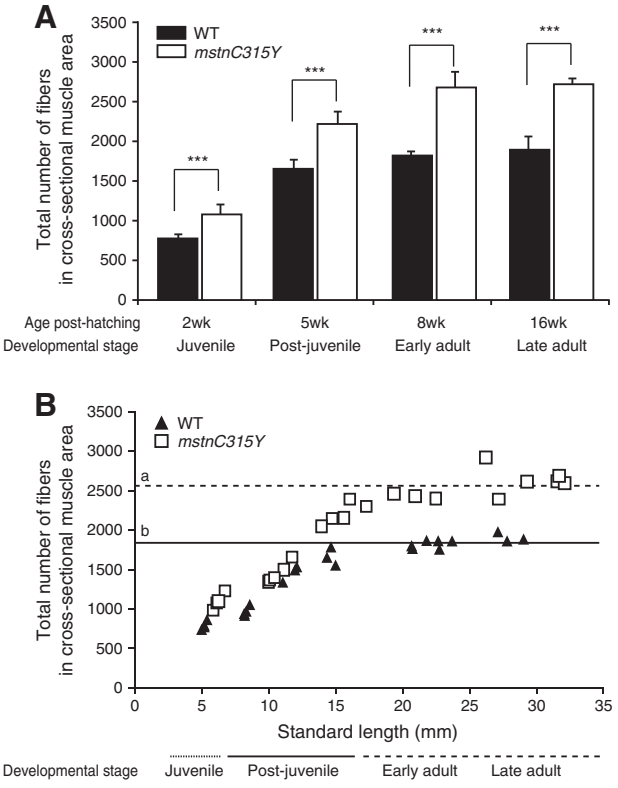

Fig. 9. Muscle fiber development in number during posthatch growth. (A) Relation between the number of fibers and age post-hatching for WT (black columns) and *mstnC315Y* (white columns) medaka. Numbers of fibers was counted in the cross-sectional muscle area, described in Fig. 5A. The number of muscle fiber in *mstnC315Y* was more than that in WT at all stages. Values are means ± SEM (n = 3, at all stages). ***$p<0.001$. (B) Relation between the number of fibers and standard length for WT (black triangles) and *mstnC315Y* (white squares). The fiber number of *mstnC315Y* per standard length was more than that of WT throughout life. Broken line *a* in panel B shows the average of plateau values in *mstnC315Y* (2551.7 ± 201.9 fibers), and black line *b* shows that in WT (1912.4 ± 129.3 fibers).

MSTN temporally controlled the expression of each MRF mRNA at each developmental stage

We investigated mRNA levels of MRFs (MyoD, Myf-5, and myogenin) in skeletal muscle between WT and *mstnC315Y*. The expression of EF-1α mRNA exhibited a steady state level at each developmental stage between WT and *mstnC315Y* medaka, resulting that EF-1α was used as a reference gene. The mRNA levels of MRFs were not significantly different between the two groups at the juvenile stage (Fig. 11A). At the post-juvenile stage, Myf-5 and MyoD mRNAs in *mstnC315Y* were expressed highly with increases of 3.4 times and 1.6 times, respectively, compared to WT (Fig. 11B). At the early adult stage, Myf-5 and MyoD mRNAs in *mstnC315Y* were kept at a high level as well as the post-juvenile stage, whereas myogenin mRNA in *mstnC315Y* was significantly increased and 4.4 times higher-expressed than WT (Fig. 11C). At the late adult stage, Myf-5 and MyoD mRNAs between WT and *mstnC315Y* were almost the same levels, whereas expression of myogenin mRNA in *mstnC315Y* was strongly up-regulated with a 10 fold increase to WT (Fig. 11D). These results showed that loss of the MSTN function induced a high-level expression of Myf-5 and MyoD from the post-juvenile stage to the early adult stage and subsequently an elevated expression of myogenin at the adult stage.

Discussion

In this study, we made MSTN mutant medaka (*mstnC315Y*), corresponding to naturally occurring mutation in double-muscled Piedmontese cattle (Kambadur et al., 1997), by using the TILLING method (Taniguchi et al., 2006). *mstnC315Y* exhibited a double-muscling phenotype with hyperplasia and hypertrophy. Hyperplasia and up-regulation of both Myf-5 and MyoD mRNA occurred at the stage from the post-juvenile to the early adult and then the hypertrophy and up-regulation of myogenin mRNA at the adult stage. These results suggested that loss of the MSTN function in the *mstnC315Y* induced hyperplasia due to up-regulation of both Myf-5 and MyoD from the post-juvenile stage to the early adult stage, and then hypertrophy due to up-regulation of myogenin at the late adult stage. The hyperplasia and hypertrophy caused an increased body weight in the *mstnC315Y*. This is the first report that loss of the MSTN function in fish causes double-muscling phenotype with both hyperplasia and hypertrophy.

The cysteine residue at the 315-position of MSTN peptide is known to be one of the important amino acid residues involved in forming the cysteine knot structure in members of the TGF-β superfamily (Berry et al., 2002). The structure is needed for a functional homodimer, which binds activin receptor type IIB (ActRIIB) to elicit a biological function (Lee and McPherron, 2001). Therefore, a point mutation at Cys (315) was fully conceivable to cause loss of the MSTN function in *mstnC315Y*. To confirm the loss of MSTN function, we analyzed smad proteins in the muscle of *mstnC315Y* and WT medaka. Smads are essential intracellular transducers for the TGF-β signaling pathway (Feng and Derynck, 2005; Shi and Massague, 2003). In response to MSTN, Smad2 and/or 3 are phosphorylated and serve as intermediate substances with the next signal transductions. In mammals *in vitro* studies, induced Smad-phosphorylations varied

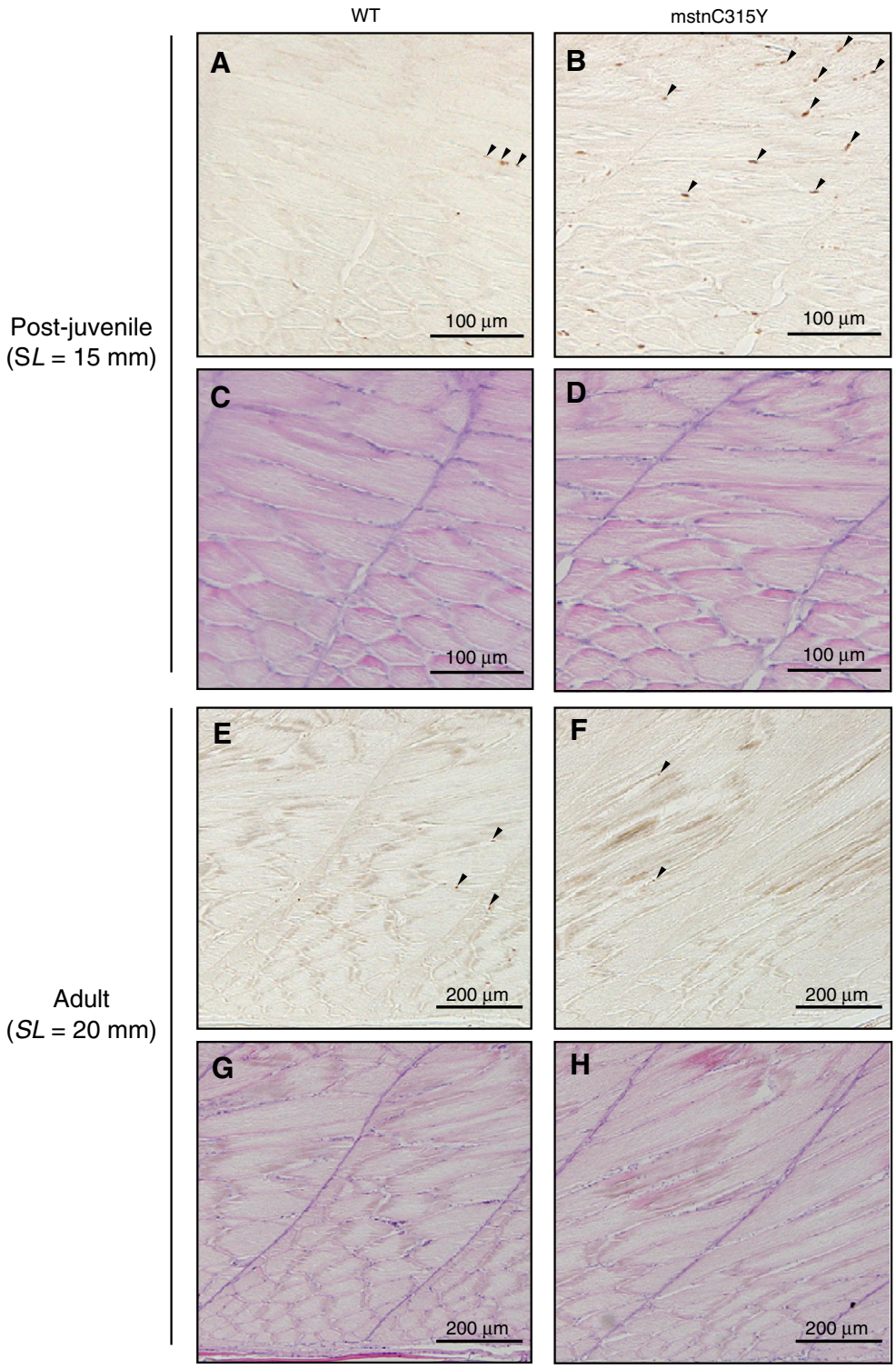

Fig. 10. Proliferation signals of myogenic cells in skeletal muscle. Immunohistochemical analysis of muscle fiber in WT (A, C, E, and G) and *mstnC315Y* (B, D, F and H) medaka. Cross-sectional area is described in Fig. 5B. Proliferation cell nuclear antigens (PCNA) were detected as described in the Materials and methods. (A to D) Muscle fibers at post-juvenile stage (*SL* = 15 mm). (A and B) PCNA-positive nuclei of cells were colored with diaminobenzine (brown). Some of the positive nuclei are indicated by arrowheads. (C and D) Sections adjacent to panels A and B for each were stained with hematoxylin–eosin. PCNA-positive nuclei were more abundant in *mstnC315Y* than in WT at the post-juvenile stage. (E to H) Muscle fibers at adult stage (*SL* = 20 mm). (E and F) PCNA-positive nuclei were colored with diaminobenzine (brown). Some of the positive nuclei are indicated by arrowheads. (G and H) Sections adjacent to panels E and F for each were stained with hematoxylin–eosin. There were few PCNA-positive nuclei in WT and *mstnC315Y*, suggesting that cell proliferation stopped in both. Scale bars; 100 μm for (A) to (D); 200 μm for (E) to (H).

with the type of cells. Recombinant MSTN protein induced only Smad3 but not Smad2 phosphorylation in C2C12 myoblasts (Langley et al., 2002), while both Smad2 and 3 phosphorylations occurred in 3T3-L1 adipocytes and 10T1/2 muscle fibroblasts (Rebbapragada et al., 2003). The phosphorylated Smad2 and/or 3 led to arrest of differentiation of these precursor cells in early differentiation. Additionally, activation of the MSTN signaling pathway induced both Smad2 and 3 phosphorylations in muscle of adult mice, resulting in inhibition of

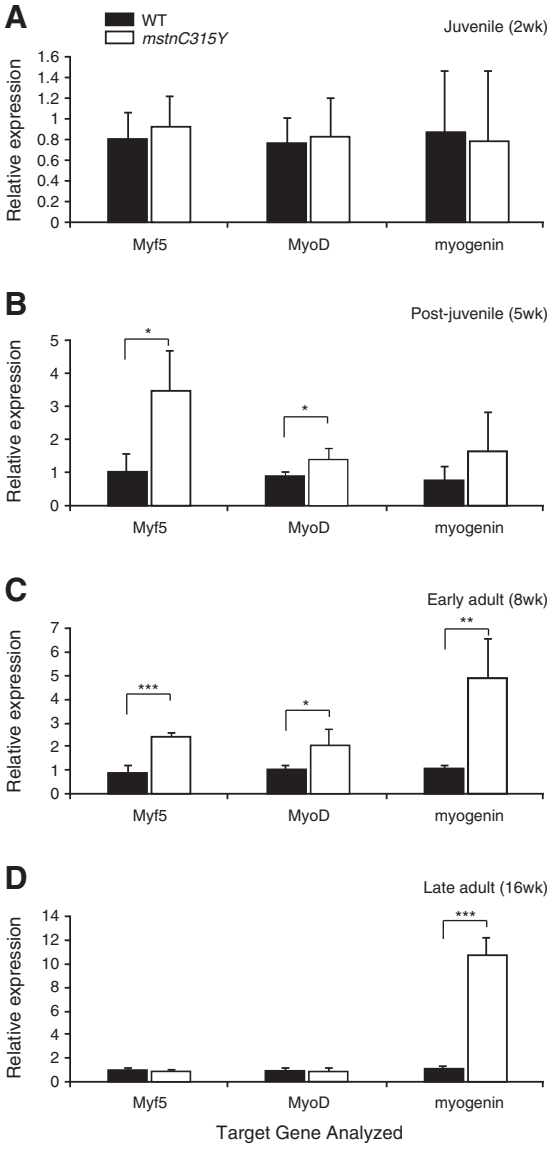

Fig. 11. Gene expression analysis of myogenic regulatory factors of skeletal muscle. Quantitative PCR analysis to measure mRNA levels of Myf-5, MyoD and myogenin in WT (black columns) and *mstnC315Y* (white columns) medaka. Expression of elongation factor 1 alpha (EF-1α) was used to normalize all samples. All relative expressions are represented as the ratio to that of WT medaka at each stage. (A) MRF expression at the juvenile stage. There was no difference in MRF expression between WT and *mstnC315Y*. (B) MRF expression at the post-juvenile stage. Myf-5 and MyoD in *mstnC315Y* were 3.4 and 1.6 times higher-expressed than those in WT. (C) MRF expression at the early adult stage. In addition to Myf-5 and MyoD, expression of myogenin in *mstnC315Y* was increased. (D) MRF expression at the late adult stage. Only myogenin was up-regulated in *mstnC315Y* with a 10 fold increase to WT. Values are means ± SEM ($n=3$, at all sample points). $^{*}p<0.05$, $^{**}p<0.01$ and $^{***}p<0.001$, respectively.

muscle hypertrophy (Sartori et al., 2009). In fish myogenesis, there have been few reports on the relation between MSTN and Smad proteins. The current study showed that nucleus extracts from WT medaka muscles at the adult stage contained phosphorylated Smad2. In contrast, *mstnC315Y* did not express phosphorylated Smad2 in the muscle. Phosphorylated Smad3 was not detected in both extracts (data not shown). These indicate that MSTN in muscle of medaka has induced Smad2 phosphorylation at the adult stage, and then the MSTN signaling pathway has been down-regulated in muscle of *mstnC315Y*. MSTN-induced phosphorylation of smads in fish muscle may be altered with developmental stages or fish species as well as previous investigations in mammals. Thus, further studies will be required to resolve this question.

One of the important factors in determining the body size in fish is the number of muscle fibers (Biga and Goetz, 2006; Veggetti et al., 1990). Our growth analysis revealed that *mstnC315Y* had a larger number of muscle fibers than WT at the post-juvenile stage although there was no difference in fiber size, indicating that the major cause of the increased body weight in *mstnC315Y* at the post-juvenile stage was only hyperplasia of muscle fibers. The growth analysis also showed that the body weight gain in *mstnC315Y* accelerated at the late post-juvenile stage, giving rise to a substantial difference in body weight between the two groups at the adult stage. One reason for this phenomenon was that hyperplasia of muscle fibers was maintained in *mstnC315Y* for a longer time. The proliferation of muscle fibers in WT stopped at the post-juvenile stage (5 wk post-hatching), whereas that in *mstnC315Y* continued to the early-adult stage (8 wk post-hatching). It was found that the extended period for proliferation of muscle fibers resulted in a large number of fibers in *mstnC315Y* at the adult stage, affecting the body weight gain at the stage. Another reason for the increasing difference in body weight was that *mstnC315Y* exhibited hypertrophy of the muscle fibers from 8 to 16 wk post-hatching compared with WT. The hypertrophy of fibers formed in *mstnC315Y*, the number of which had already been more than that of WT, further led to the widening difference in body weight. Therefore, our investigation throughout the life in medaka showed that hypermorphosis of skeletal muscle in *mstnC315Y* was due to the development of fibers through the hyperplasia phase, followed by the hypertrophy phase. This sequential hypermorphosis in fibers was responsible for the increased body weight of *mstnC315Y*.

Comparing the myogenesis in *mstnC315Y* with WT throughout life, we found that muscle fiber development in medaka altered during posthatch growth. Also in mammals, the differentiation pattern in muscle fiber varies at development stages (Rowe and Goldspink, 1969; White et al., 2010); however, it should be noted that the changing point of the differentiation pattern differs between medaka and mammals. In mammals, myogenic cell proliferation was stopped by the MSTN signaling pathway at the late-prenatal stage (Amthor et al., 2009; Manceau et al., 2008) and skeletal muscles achieve nearly a full complement of muscle fibers before birth (White et al., 2010). Muscle growth at the postnatal stage can be accomplished by an increase in the size of individual muscle fibers, except for muscle repair. Therefore in mammals, the differentiation pattern in muscle fibers changes prior to birth. Our study showed that muscle fibers in medaka were able to grow with an increase in number and size during posthatch growth. Our data also shows that an increase in size of muscle fiber occurred only in the adult stage in medaka, indicating that the pattern of differentiation in muscle fibers alters at the adult stage. These indicate that myogenesis in medaka at the adult stage corresponds to postnatal myogenesis in mammals in terms of the differentiation pattern in fibers. Based on the data in this study, we propose that medaka can be utilized to analyze myogenesis. As a model animal of postnatal mammal, adult stage medaka can be utilized to analyze myogenesis. Additionally, medaka from the embryonic stage to the post-juvenile stage can be analyzed as a model animal of prenatal mammal. In fish, unlike mammals, muscle growth with both hyperplasia and hypertrophy can continue throughout life; however, our data showed that the pattern of differentiation in muscle fibers of medaka was clearly differentiated. Therefore, if medaka as a model fish is used to analyze fish myogenesis, it should be treated with particular attention in regards to muscle fiber development.

In general, while tissues used in previous studies on mammalian skeletal myogenesis had been muscles of arms or legs, skeletal muscle in fish, except for fin muscles, correspond to the body trunk in mammals (Burke and Nowicki, 2003). Despite differences in the derivation of muscle, we found that the MRF-mediated mechanism for muscle fiber formation was conserved between skeletal muscle in medaka and muscles of the limbs in mammals. In mammals, Myf-5 and MyoD activate satellite cells (stem cells of myoblasts), and then

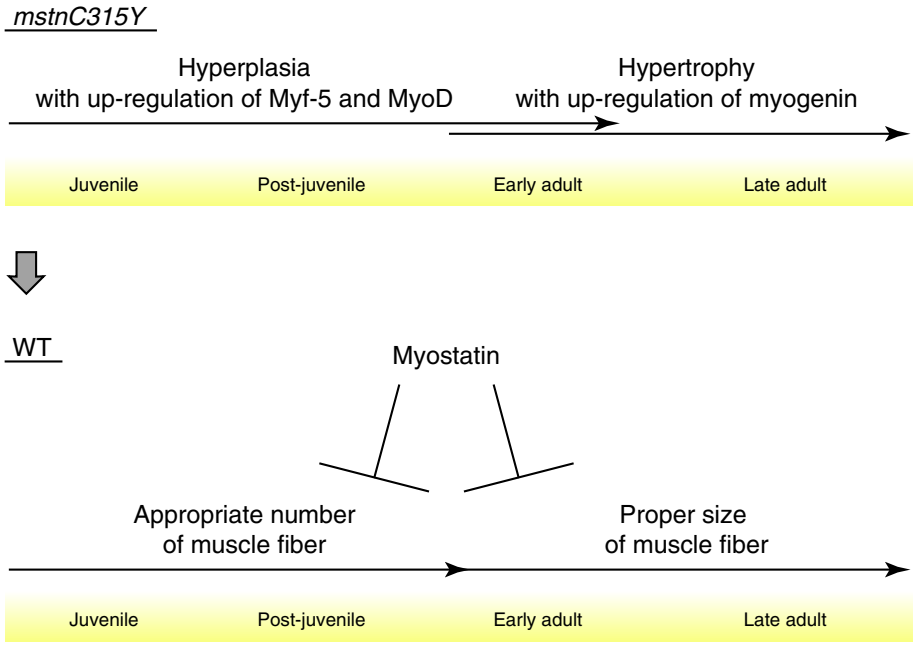

Fig. 12. Model summarizing the inhibitory roles of MSTN in medaka during post-hatch growth. In *mstnC315Y*, hyperplasia occurred until the early adult stage with up-regulations of Myf-5 and MyoD, and then hypertrophy was induced at the adult stage with up-regulation of myogenin. These indicate that MSTN in medaka plays an inhibitory role for hyperplastic growth in muscle fiber during the juvenile and post-juvenile stages, followed by another inhibitory role for hypertrophic growth in muscle fiber at the adult stage.

induce differentiation of those into myoblasts in cultured myogenic cells (Kablar et al., 1997; Olson and Klein, 1994). Myf-5 and MyoD are also essential factors for the successful proliferation of muscle fibers during hyperplasia at postnatal myogenesis (Oldham et al., 2001). Myogenin is critical in the late phase of muscle differentiation specifically during the terminal differentiation at embryonic myogenesis and hypertrophy at postnatal myogenesis (Olson and Klein, 1994; Venuti et al., 1995). MRFs that were initially isolated in mammals are also present in the genome of fish (Rescan, 2001). There has been minimal study of relation between MRFs and myogenesis at the posthatch stage, although several reports showed that MRFs in fish play a role similar to those in mammals in embryonic somitogenesis (Amali et al., 2004; Hinits et al., 2009). In our analysis, the expression pattern for MRF mRNAs in *mstnC315Y* was consistent with the phenotype of muscle fiber development during posthatch growth. Hyperplasia occurred with the high expression of both Myf-5 and MyoD, and then hypertrophy occurred with the high expression of myogenin. These indicate that MRFs in medaka could be available as myogenic markers at the posthatch stage.

In this study we had expected that all MRFs in *mstnC315Y* were expressed at high levels all through the developmental stages, since muscle in fish can grow during the posthatch period and the MSTN signaling pathway in *mstnC315Y* was fully inhibited. Contrary to our hypothesis, the expression of Myf-5 and MyoD were suppressed and the expression of myogenin was accelerated at the same time (from 8 to 16 wk post hatching) in *mstnC315Y*. At present, we have one explanation to resolve the contradiction. It's to be noted that the insulin-like growth factor (IGF) is also an important factor involved in myogenesis. Florini et al. reported that IGF-1 regulated MRFs indirectly to enable skeletal muscle development (Florini et al., 1996). That is, IGF-1-activated the ERK (extracellular signal-related kinase) signaling pathway inhibiting Myf-5 and MyoD expression and activity (Miyake et al., 2007). Furthermore, IGF-1-induced PI3K/Akt (phosphoinositide-3 kinase/ protein kinase B) signaling pathway promotes the expression of myogenin (Miyake et al., 2007; Serra et al., 2007). In fish, several reports have revealed that the expression of IGF-1 was up-regulated as sexual maturation (puberty) began (Le Gac et al., 2001; Maestro et al., 1997; Onuma et al., 2010). Since the period from 5 to 8 wk post-hatching in medaka includes the onset of sexual maturation, it remains possible that not only MSTN, but also IGF-1 is related with high expressions of MRFs in *mstnC315Y*.

Finally, the roles of MSTN in muscle fiber development of medaka are illustrated in Fig. 12. MSTN mutant medaka *mstnC315Y* shows a body weight gain with hyperplasia and hypertrophy during posthatch growth. Hyperplasia in *mstnC315Y* occurred from the post-juvenile stage to the early adult stage with the high expression of both Myf-5 and MyoD. Hypertrophy in *mstnC315Y* was induced at the adult stage with the high expression of myogenin. These indicated that MSTN in medaka plays a dual role in muscle fiber development, which is an inhibitory role in hyperplastic growth at the post-juvenile stage, and hypertrophic growth at the adult stage. In conclusion, MSTN in medaka regulates the number and size of muscle fiber in a temporally controlled manner during posthatch growth.

Acknowledgments

We would like to thank Miwa Osa and Atsuko Matsumoto (NRIA) for the assistance during the experiment. This work was supported by the Program for Promotion of Basic and Applied Researches for Innovations in Bio-oriented Industry (BRAIN), Japan.

References

Amali, A.A., Lin, C.J., Chen, Y.H., Wang, W.L., Gong, H.Y., Lee, C.Y., Ko, Y.L., Lu, J.K., Her, G.M., Chen, T.T., Wu, J.L., 2004. Up-regulation of muscle-specific transcription factors during embryonic somitogenesis of zebrafish (*Danio rerio*) by knock-down of myostatin-1. Dev. Dyn. 229, 847–856.

Amthor, H., Otto, A., Vulin, A., Rochat, A., Dumonceaux, J., Garcia, L., Mouisel, E., Hourde, C., Macharia, R., Friedrichs, M., Relaix, F., Zammit, P.S., Matsakas, A., Patel, K., Partridge, T., 2009. Muscle hypertrophy driven by myostatin blockade does not require stem/precursor-cell activity. Proc. Natl. Acad. Sci. U. S. A. 106, 7479–7484.

Berry, C., Thomas, M., Langley, B., Sharma, M., Kambadur, R., 2002. Single cysteine to tyrosine transition inactivates the growth inhibitory function of Piedmontese myostatin. Am. J. Physiol. Cell Physiol. 283, C135–C141.

Biga, P.R., Goetz, F.W., 2006. Zebrafish and giant *Danio* as models for muscle growth: determinate vs. indeterminate growth as determined by morphometric analysis. Am. J. Physiol. Regul. Integr. Comp. Physiol. 291, R1327–R1337.

Burke, A.C., Nowicki, J.L., 2003. A new view of patterning domains in the vertebrate mesoderm. Dev. Cell 4, 159–165.

Bustin, S.A., Benes, V., Garson, J.A., Hellemans, J., Huggett, J., Kubista, M., Muller, R., Nolan, T., Pfaffl, M.W., Shipley, G.L., Vandesompele, J., Wittwer, C.T., 2009. The MIQE guidelines: minimum information for publication of quantitative real-time PCR experiments. Clin. Chem. 4, 611–622.

Delgado, I., Fuentes, E., Escobar, S., Navarro, C., Corbeaux, T., Reyes, A.E., Vera, M.I., Alvarez, M., Molina, A., 2008. Temporal and spatial expression pattern of the myostatin gene during larval and juvenile stages of the Chilean flounder (*Paralichthys adspersus*). Comp. Biochem. Physiol. B. Biochem. Mol. Biol. 151, 197–202.

Feng, X.H., Derynck, R., 2005. Specificity and versatility in tgf-beta signaling through Smads. Annu. Rev. Cell Dev. Biol. 21, 659–693.

Florini, J.R., Ewton, D.Z., Coolican, S.A., 1996. Growth hormone and the insulin-like growth factor system in myogenesis. Endocr. Rev. 17, 481–517.

Hinits, Y., Osborn, D.P., Hughes, S.M., 2009. Differential requirements for myogenic regulatory factors distinguish medial and lateral somitic, cranial and fin muscle fibre populations. Development 136, 403–414.

Johnston, I.A., 1999. Muscle development and growth: potential implications for flesh quality in fish. Aquaculture 177, 99–115.

Kablar, B., Krastel, K., Ying, C., Asakura, A., Tapscott, S.J., Rudnicki, M.A., 1997. MyoD and Myf-5 differentially regulate the development of limb versus trunk skeletal muscle. Development 124, 4729–4738.

Kambadur, R., Sharma, M., Smith, T.P., Bass, J.J., 1997. Mutations in *myostatin* (GDF8) in double-muscled Belgian Blue and Piedmontese cattle. Genome Res. 7, 910–916.

Kimori, Y., Oguchi, Y., Ichise, N., Baba, N., Katayama, E., 2007. A procedure to analyze surface profiles of the protein molecules visualized by quick-freeze deep-etch replica electron microscopy. Ultramicroscopy 107, 25–39.

Kimori, Y., Baba, N., Morone, N., 2010. Extended morphological processing: a practical method for automatic spot detection of biological markers from microscopic images. BMC Bioinforma. 11, 373.

Langley, B., Thomas, M., Bishop, A., Sharma, M., Gilmour, S., Kambadur, R., 2002. Myostatin inhibits myoblast differentiation by down-regulating MyoD expression. J. Biol. Chem. 277, 49831–49840.

Le Gac, F., Thomas, J.L., Mourot, B., Loir, M., 2001. In vivo and in vitro effects of prochloraz and nonylphenol ethoxylates on trout spermatogenesis. Aquat. Toxicol. 53, 187–200.

Lee, S.J., McPherron, A.C., 2001. Regulation of myostatin activity and muscle growth. Proc. Natl. Acad. Sci. U. S. A. 98, 9306–9311.

Lee, C.Y., Hu, S.Y., Gong, H.Y., Chen, M.H., Lu, J.K., Wu, J.L., 2009. Suppression of myostatin with vector-based RNA interference causes a double-muscle effect in transgenic zebrafish. Biochem. Biophys. Res. Commun. 387, 766–771.

Lizotte, E., Tremblay, A., Allen, B.G., Fiset, C., 2005. Isolation and characterization of subcellular protein fractions from mouse heart. Anal. Biochem. 345, 47–54.

Maestro, M.A., Planas, J.V., Moriyama, S., Gutierrez, J., Planas, J., Swanson, P., 1997. Ovarian receptors for insulin and insulin-like growth factor I (IGF-I) and effects of IGF-I on steroid production by isolated follicular layers of the preovulatory coho salmon ovarian follicle. Gen. Comp. Endocrinol. 106, 189–201.

Manceau, M., Gros, J., Savage, K., Thome, V., McPherron, A., Paterson, B., Marcelle, C., 2008. Myostatin promotes the terminal differentiation of embryonic muscle progenitors. Genes Dev. 22, 668–681.

McPherron, A.C., Lee, S.J., 1997. Double muscling in cattle due to mutations in the myostatin gene. Proc. Natl. Acad. Sci. U. S. A. 94, 12457–12461.

McPherron, A.C., Lawler, A.M., Lee, S.J., 1997. Regulation of skeletal muscle mass in mice by a new TGF-beta superfamily member. Nature 387, 83–90.

Meyer, F., 1979. Iterative image transformations for an automatic screening of cervical smears. J. Histochem. Cytochem. 27, 128–135.

Meyer, F., Beucher, S., 1990. Morphological segmentation. J. Visual. Commun. Image Represent. 1, 21–46.

Miyake, M., Hayashi, S., Sato, T., Taketa, Y., Watanabe, K., Tanaka, S., Ohwada, S., Aso, H., Yamaguchi, T., 2007. Myostatin and MyoD family expression in skeletal muscle of IGF-1 knockout mice. Cell Biol. Int. 31, 1274–1279.

Mosher, D.S., Quignon, P., Bustamante, C.D., Sutter, N.B., Mellersh, C.S., Parker, H.G., Ostrander, E.A., 2007. A mutation in the myostatin gene increases muscle mass and enhances racing performance in heterozygote dogs. PLoS Genet. 3, e79.

Niblack, W., 1986. An Introduction to Digital Image Processing. Prentice Hall, pp. 115–116.

Oldham, J.M., Martyn, J.A., Sharma, M., Jeanplong, F., Kambadur, R., Bass, J.J., 2001. Molecular expression of myostatin and MyoD is greater in double-muscled than normal-muscled cattle fetuses. Am. J. Physiol. Regul. Integr. Comp. Physiol. 280, R1488–R1493.

Olson, E.N., Klein, W.H., 1994. bHLH factors in muscle development: dead lines and commitments, what to leave in and what to leave out. Genes Dev. 8, 1–8.

Onuma, T.A., Makino, K., Katsumata, H., Beckman, B.R., Ban, M., Ando, H., Fukuwaka, M.A., Azumaya, T., Swanson, P., Urano, A., 2010. Changes in the plasma levels of insulin-like growth factor-I from the onset of spawning migration through upstream migration in chum salmon. Gen. Comp. Endocrinol. 165, 237–243.

Pfaffl, M.W., 2001. A new mathematical model for relative quantification in real-time RT-PCR. Nucleic Acids Res. 29, e45.

Rebbapragada, A., Benchabane, H., Wrana, J.L., Celeste, A.J., Attisano, L., 2003. Myostatin signals through a transforming growth factor beta-like signaling pathway to block adipogenesis. Mol. Cell. Biol. 23, 7230–7242.

Rescan, P.Y., 2001. Regulation and functions of myogenic regulatory factors in lower vertebrates. Comp. Biochem. Physiol. B. Biochem. Mol. Biol. 130, 1–12.

Rowe, R.W., Goldspink, G., 1969. Muscle fibre growth in five different muscles in both sexes of mice. J. Anat. 104, 519–530.

Sartori, R., Milan, G., Patron, M., Mammucari, C., Blaauw, B., Abraham, R., Sandri, M., 2009. Smad2 and 3 transcription factors control muscle mass in adulthood. Am. J. Physiol. Cell. Physiol. 296, C1248–C1257.

Sawatari, E., Seki, R., Adachi, T., Hashimoto, H., Uji, S., Wakamatsu, Y., Nakata, T., Kinoshita, M., 2010. Overexpression of the dominant-negative form of myostatin results in doubling of muscle-fiber number in transgenic medaka (*Oryzias latipes*). Comp. Biochem. Physiol. A. Mol. Integr. Physiol. 155, 183–189.

Schuelke, M., Wagner, K.R., Stolz, L.E., Hubner, C., Riebel, T., Komen, W., Braun, T., Tobin, J.F., Lee, S.J., 2004. Myostatin mutation associated with gross muscle hypertrophy in a child. N. Engl. J. Med. 350, 2682–2688.

Serra, C., Palacios, D., Mozzetta, C., Forcales, S.V., Morantte, I., Ripani, M., Jones, D.R., Du, K., Jhala, U.S., Simone, C., Puri, P.L., 2007. Functional interdependence at the chromatin level between the MKK6/p38 and IGF1/PI3K/AKT pathways during muscle differentiation. Mol. Cell 28, 200–213.

Shi, Y., Massague, J., 2003. Mechanisms of TGF-beta signaling from cell membrane to the nucleus. Cell 113, 685–700.

Taniguchi, Y., Takeda, S., Furutani-Seiki, M., Kamei, Y., Todo, T., Sasado, T., Deguchi, T., Kondoh, H., Mudde, J., Yamazoe, M., Hidaka, M., Mitani, H., Toyoda, A., Sakaki, Y., Plasterk, R.H., Cuppen, E., 2006. Generation of medaka gene knockout models by target-selected mutagenesis. Genome Biol. 7, R116.

Veggetti, A., Mascarello, F., Scapolo, P.A., Rowlerson, A., 1990. Hyperplastic and hypertrophic growth of lateral muscle in *Dicentrarchus labrax* (L.). An ultrastructural and morphometric study. Anat. Embryol (Berl) 182, 1–10.

Venuti, J.M., Morris, J.H., Vivian, J.L., Olson, E.N., Klein, W.H., 1995. Myogenin is required for late but not early aspects of myogenesis during mouse development. J. Cell Biol. 128, 563–576.

White, R.B., Bierinx, A.S., Gnocchi, V.F., Zammit, P.S., 2010. Dynamics of muscle fibre growth during postnatal mouse development. BMC Dev. Biol. 10, 21.

Xu, C., Wu, G., Zohar, Y., Du, S.J., 2003. Analysis of *myostatin* gene structure, expression and function in zebrafish. J. Exp. Biol. 206, 4067–4079.